RAPID COMMUNICATIONS

PHYSICAL REVIEW B VOLUME 33, NUMBER 6 15 MARCH 1986

# Modulated-reflectance spectroscopy of InP doping superlattices

M. Gal, J. S. Yuan, J. M. Viner, P. C. Taylor, and G. B. Stringfellow
*Department of Physics and Department of Materials Science and Engineering, University of Utah, Salt Lake City, Utah 84112*
(Received 27 January 1986)

Photoreflectance (PR) measurements in doping superlattices show that the photoexcited carriers modulate the subband levels in a very predictable fashion. We demonstrate the utility of the PR technique for probing details of quantum-size effects in doping superlattices.

Electroreflectance (ER) and photoreflectance (PR) are valuable and venerable techniques for understanding interband transitions in bulk semiconductors. However, detailed line-shape analyses are difficult for bulk semiconductors because the modulation of the reflection is caused by surface fields which are often hard to characterize.[1-3] Recently, there have been several applications of the ER[4,5] and PR[6] techniques to semiconductor superlattices, or quantum-well structures, mainly in the GaAs-$Ga_{1-x}Al_xAs$ system. Here again, although a wealth of information can be obtained concerning characteristic energies for the various interband transitions, detailed line-shape analyses are complicated by a variety of factors including the nature of the electric fields and the presence of overlapping transitions of different types.

The PR technique is very similar to the well-known electromodulation technique, which produces derivativelike features in the reflectivity spectra near the vicinity of the interband transitions. PR, which can easily be performed at room temperature, can be considered as a contactless form of electromodulation in which the modulation is produced by the photoinjected carriers.

This paper describes the first application of the PR technique to doping superlattices, which are structures consisting of alternate layers of *n*- and *p*-doped semiconductor (so-called *n-i-p-i* structures).[7] This class of superlattices has a tunable optical band gap, which depends on the free-carrier concentration, and extremely long minority-carrier lifetimes due to the spatial separation between electrons and holes in the *n* and *p* layers. In addition to these unique features, the *n-i-p-i* superlattices also exhibit quantum-size effects similar to those observed in quantum wells. The first observation of quantized subbands in GaAs-$Ga_{1-x}Al_xAs$ doping superlattices was achieved by resonant spin-flip Raman scattering (RRS).[8] However, with the development of superlattices which are not based on GaAs, RRS can become extremely difficult, due to the lack of resonant laser lines.

Because optical modulation in the doping superlattices affects the real-space modulation of the band gap and the population of the subband levels in a very predictable fashion,[7,9] a detailed and semiquantitative understanding can be obtained. The optical modulation with light of energy greater than the band-gap energy produces electrons and holes which modulate the electric fields generated in the superlattice by the spatial distribution of the dopants. This effect, in turn, modulates the position of the electronic subbands in the conduction band and contributes to a modulation of the reflectivity in the vicinity of these subband levels. The PR spectra permit us to identify the allowed transitions between the valence band and quantized subbands of the conduction band. The results presented below for InP doping superlattices[10] illustrate the potential of the PR technique for probing quantum confinement in these layer structures.

Besides the initial work on GaAs doping superlattices grown by molecular-beam epitaxy (MBE),[11-13] InP *n-i-p-i* structures have recently been fabricated using vapor-phase epitaxial (VPE) techniques.[14] We have reported the first InP doping superlattices grown by the organometallic VPE (OMVPE) technique.[10] In the InP doping superlattices grown by OMVPE, the peak energy and the line shape of the photoluminescence (PL) spectra were found to depend on the excitation intensity just as predicted theoretically. The time decay of the luminescence contained distinct steps, indicating the existence of subbands due to quantum-size effects.[10]

The samples used in this study were made by the OMVPE technique. Sample preparation procedures have been described in detail elsewhere.[10,15] Samples were grown at a rate of 0.1 $\mu$m/min. The *n* and *p* layers were grown for approximately 7–50 s with an interruption of the growth of approximately 30 s between layers to produce abrupt doping profiles. The samples consisted of six 200-Å layers with doping levels of $1\times10^{18}$ and $2\times10^{18}$ $cm^{-3}$ for the *n* and *p* layers. Layer thicknesses were determined from the known growth rates.[10] Doping levels were determined from the dopant partial pressures during growth and Hall effect measurements on thick layers were employed to calibrate the dopant distribution coefficient.[10] The experimental arrangement of the PR technique is very similar to that described in the literature.[3] The modulation source was an argon-ion laser, the intensity of which was modulated at 350 Hz. The modulation intensity was varied using neutral-density filters.

Figure 1 shows the PR spectrum of an InP doping superlattice at 80 K using 1.2 $W cm^{-2}$ at 2.41 eV (5145 Å) as the modulation source. A corresponding spectrum at 300 K is shown in Fig. 2. Above the bulk band gap of InP ($E_g^0$), several PR lines are observed in both of these figures. Unlike the case of PR in bulk semiconductors, these lines are strongly dependent on the modulated light intensity as shown in Fig. 3. At lower intensities the PR lines become narrower and additional features appear (Fig. 3). These features, which we will show are due to transitions between the valence band (and the split-off valence band) and the quantized subbands of the conduction band, can be calculated using known expressions for doping superlattices.[9] (The weak and sharp features in Fig. 3 are due to noise.)

 

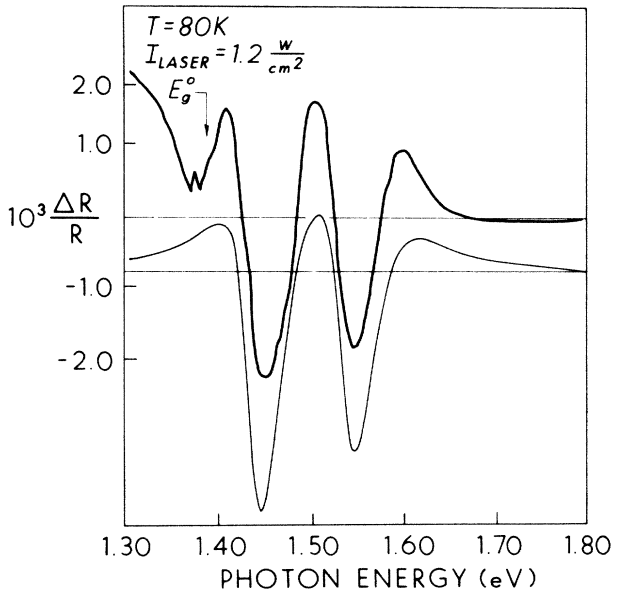


FIG. 1. Low-temperature (80 K) PR spectrum at high modulation intensity in an InP doping superlattice. $E_g^0$ denotes the band gap of bulk InP. The lower trace is a calculated spectrum based on the model described in the text.

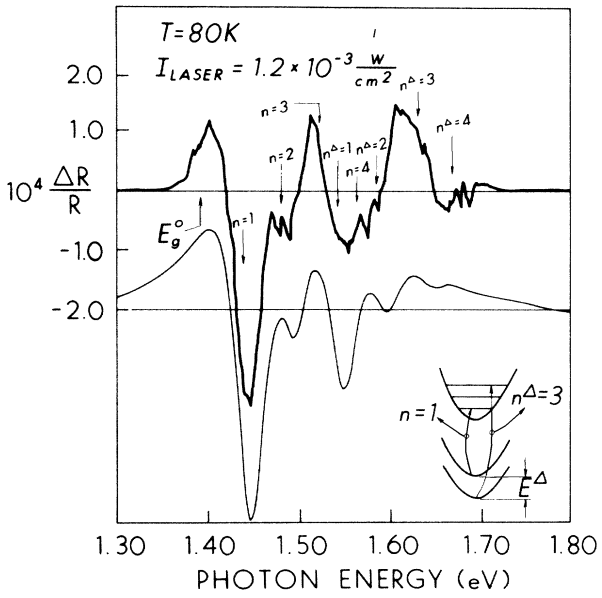


FIG. 3. Low-temperature (80 K) PR spectrum at low modulation intensity in an InP doping superlattice. $E_g^0$ denotes the band gap of bulk InP. The indices $n$ and $n^\Delta$ refer to transitions from, respectively, the valence band and the split-off valence band to the subband levels in the conduction band. The lower trace is a calculated spectrum based on the model described in the text.

The weak structure near and below $\sim 140$ eV is due to the well-known $E_0$ transition in the bulk InP substrate. Although the observed structure is weak, it was consistently observed at all temperatures and for all samples at the $E_0$ point of bulk InP. At 77 K the laser modulation, besides modulating the reflectivity, also excites below band-gap PL, which at the given intensity peaked at 1.26 eV.[10] The structure in Fig. 1 in $\Delta R/R$ at low energies ($\lesssim 1.35$ eV) is due to this PL from the doping-superlattice structure.[10] Note from Fig. 2 that at room temperature the PL is unobservable and the PR lines shift to lower energy.

For the sample used in Figs. 1–3 we calculate that there will be at most five quantized levels in the conduction band with the existence of the fifth-level problematical because of uncertainties in the values of the experimental parameters. The situation is shown schematically in the inset of Fig. 3.

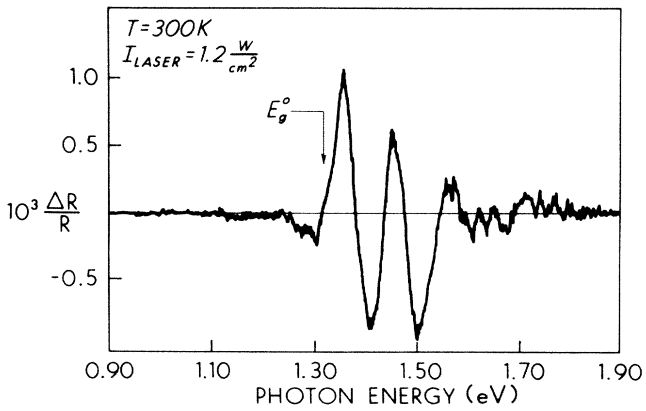


FIG. 2. Room-temperature PR spectrum at high modulation intensity in an InP doping superlattice.

The quantity $E^\Delta$ is the energy difference between the valence band and the split-off valence band, and transitions from the valence band and split-off valence band to the subband levels of the conduction band are denoted by the indices $n$ and $n^\Delta$, respectively. (We ignore the quantized subbands in the valence band because their splittings in InP are an order of magnitude smaller than those of the conduction band.) The transition energies are given by[9]

$$E^n = E_g^0 + E_c^n , \tag{1}$$

where

$$E_c^n = h\left(\frac{4\pi e^2 N_D}{\kappa_0 m_c^*}\right)^{1/2} (n+\tfrac{1}{2}), \quad n = 0, 1, \ldots , \tag{2}$$

and where we have ignored the contribution due to subbands in the valence band. In Eq. (1) $E_g^0$ is the band-gap energy of bulk InP and $E_c^n$ is the energy of the $n$th subband level with respect to the conduction-band minimum. In Eq. (2) $N_D$ is the donor concentration, $\kappa_0$ the low-frequency dielectric constant, and $m_c^*$ the conduction-band effective mass.

Equation (2) predicts a shift in the subband levels with doping which depends on $N_D^{1/2}$. As shown in Fig. 4, this shift is observed in the PR spectra. Superimposed in Fig. 4 are the $n=1$ transitions at low modulation intensity for two samples which are equivalent, except for $N_D \sim 1\times 10^{18}$ and $2\times 10^{18}$ cm$^{-3}$, respectively. The observed shift of $\sim 15$ meV is consistent with the predictions of Eq. (2) which yields 19 meV for this case.

For the sample whose results are displayed in Figs. 1–3, the appropriate parameters for Eqs. (1) and (2) are $E^\Delta = 0.11$ eV, $2E_c^0 = 46$ meV, and $E_g^0 = 1.41$ eV at 80 K (1.31 eV at 300 K). The positions of the various transitions at 80 K are shown in Fig. 3. It is not immediately apparent

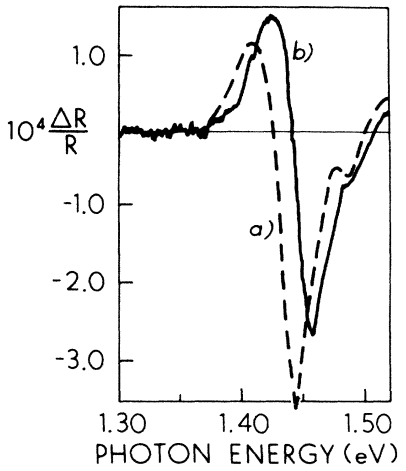


FIG. 4. Comparison of low-energy portions of room-temperature PR spectra at $\sim 1$ mW cm$^{-2}$ modulation intensity for two doping superlattices of different doping concentrations. (a) $N_D \sim 1\times10^{18}$ cm$^{-3}$, (b) $N_D \sim 2\times10^{18}$ cm$^{-3}$. See text for details.

that the observed spectral features in Fig. 3 are adequately explained by the transitions as listed. For this reason we have calculated the expected line shape using a simple model of Lorentzian oscillators which was originally developed for ER of excitons.[16] If the transition to the $n$th subband is characterized by an oscillator strength $f_n$ and occurs at energy $\hbar\bar{\omega}_n$, then the normalized change in the reflectivity due to a modulation of the $n$th subband energy can be expressed as[16]

$$\frac{\Delta R}{R} \propto \sum_n |f_n|^2 \Gamma_n^{-3} \left[ \frac{w^2(n)-1}{[w^2(n)+1]^2} \right], \tag{3}$$

where

$$w(n) = \left[ \frac{2}{\Gamma_n} \right] (\omega - \bar{\omega}_n), \tag{4}$$

and where $\Gamma_n$ is a broadening parameter (linewidth). We ignore the contribution to the PR line shape due to any modulation of the broadening parameter because the subband energies are known to be a strong function of the light intensity,[11-13] and this effect should dominate the line shapes in the doping superlattices. It is interesting to note that the line shapes associated with each transition are very similar to those observed in ER and PR of bulk semiconductors in the high-field regime.[1,2] However, the total PR spectrum is more complicated than ER in bulk InP because of the contribution from several different subbands.

The oscillator strengths $f_n$ are not easily calculable, but several general comments can be made. The matrix elements, which describe the overlap between the harmonic oscillator states in the subbands of the conduction band $[e^{-x^2/2}H_n(x)]$ and excited states in the valence band (which can be expressed as superpositions of plane waves), involve integrals of the form

$$\int dx e^{-x^2/2} H_n(x) e^{ikx}.$$

Because the specific values for the transition probabilities depend on the details of the valence-band wave functions, one may use the experimental data of Fig. 3 to investigate details of these wave functions. For the perfectly symmetric situation, one would expect only even harmonic oscillator functions to contribute, which would result in the observation of every other subband. However, we observe contributions to $\Delta R/R$ from all subband levels. This fact means that there is an asymmetry in the modulated structure which is sufficient to relax completely this selection rule. We believe that this situation results from an asymmetry in the doping profile which is inherent in the growth procedure. The experimental data suggest that the oscillator strengths are a relatively weak function of $n$.

If the important wave vectors of the valence-band states were known, one could calculate[17] the ratio of the transition probabilities to the various harmonic oscillator levels. Since little is known concerning these excited levels in the valence band, we have fit the spectrum in Fig. 3 with the $n=0$ to four levels roughly in the ratio of $1/(n+1)$ and with $\Gamma_n = 0.027$. The transitions from the split-off valence band ($n^\Delta$) were taken to be 0.5 of those from the valence band ($n$). One should not place too much emphasis on the intensities of the various transitions for this somewhat arbitrary choice of transition probabilities. On the other hand, the calculated inflection points, which correspond closely to those observed experimentally, are essentially independent of the $n$ dependence of the transition probabilities.

At higher light modulation intensities the energy separations between subbands decrease logarithmically.[18] [Equation (2) applies only for infinitesimally small modulation intensity.] Figure 1 shows the line shape calculated with essentially the same parameters used in the low-intensity curve of Fig. 3 but with $2E_c^0 = 18$ meV as the theoretical calculations indicate.[19] (The ratio of the transitions $n$ and $n^\Delta$ was taken as 1:0.8 in this case.) The experimental trace is accurately reproduced in the model calculation.

Attempts to observe PR lines in undoped, ultrahigh purity bulk InP, as well as in $n$- and $p$-doped layers with various doping levels, were unsuccessful. These results are not surprising, considering the fact that the surface electric fields in InP are well known to be small in comparison to GaAs.[19] The null results on bulk InP also reinforce the conclusion that the PR results in the doping superlattices are due to modulation of the subbands of the conduction band.

In summary, we have demonstrated the great potential of the PR technique for studying quantum-size effects in doping superlattices. The observed PR line shapes are well explained by photomodulation of the subbands in the conduction band. More extensive studies may yield detailed information concerning electronic wave functions, both for excited states near the valence-band maximum (in real space) and for the quantized subbands of the conduction band.

The authors gratefully acknowledge several very useful discussions with D. L. Mattis. The research of two of us (J.S.Y. and G.B.S.) in the Department of Materials Science and Engineering was supported by the U. S. Army Research Office, under Contract No. DAAG20-83-K-0153. The research of two of us (P.C.T. and J.M.V.) in the Department of Physics was supported by the U. S. Office of Naval Research under Contract No. N00014-83-0535 and one of us (M.G.) by the National Science Foundation under Grant No. DMR-83-04471.

[1]D. E. Aspnes and A. Frova, Phys. Rev. B **2**, 1037 (1970).
[2]D. E. Aspnes, Solid State Commun. **8**, 267 (1970).
[3]J. L. Shay, Phys. Rev. B **2**, 803 (1970).
[4]E. E. Mendez, L. L. Chang, G. Landgren, R. Ludeke, and L. Esaki, Phys. Rev. Lett. **46**, 1230 (1981).
[5]M. Erman, J. B. Theeten, P. Frijlink, S. Gaillard, F. J. Hia, and C. Alibert, J. Appl. Phys. **56**, 3241 (1984).
[6]O. J. Glembocki, B. V. Shanabrook, N. Bottka, W. T. Beard, and J. Comas, Appl. Phys. Lett. **46**, 970 (1985).
[7]G. H. Döhler, Phys. Status Solidi (b) **52**, 79 (1972); **52**, 533 (1972).
[8]J. E. Zucker, A. Pinczuk, D. S. Chemla, A. Gossard, and W. Wiegmann, Phys. Rev. Lett. **51**, 1293 (1983).
[9]G. H. Döhler, J. Vac. Sci. Technol. B **1**, 278 (1983).
[10]J. S. Yuan, M. Gal, P. C. Taylor, and G. B. Stringfellow, Appl. Phys. Lett. **47**, 405 (1985).
[11]K. Ploog, Annu. Rev. Mater. Sci. **12**, 123 (1982).
[12]H. Jung, H. Kunzel, G. H. Döhler, and K. Ploog, J. Appl. Phys. **54**, 6965 (1983).
[13]Y. Horikoshi, A. Fischer, and K. Ploog, Appl. Phys. Lett. **45**, 919 (1984).
[14]Y. Yamauchi, K. Uwai, and O. Mikami, Jpn. J. Appl. Phys. **23**, L785 (1984).
[15]C. P. Kuo, J. S. Yuan, R. M. Cohen, J. Dunn, and G. B. Stringfellow, Appl. Phys. Lett. **44**, 550 (1984).
[16]M. Cardona, in *Modulation Spectroscopy,* Solid State Physics, Suppl. 11, edited by F. Seitz, D. Turnbull, and H. Ehrenreich (Academic, New York, 1964), p. 110.
[17]The authors are indebted to D. L. Mattis for calculating the transition probabilities for representative choices of valence-band wave functions.
[18]G. H. Döhler, H. Künzel, D. Olego, K. Ploog, P. Ruden, and H. J. Stolz, Phys. Rev. Lett. **47**, 864 (1981).
[19]H. H. Wieder, Surf. Sci. **132**, 390 (1983).